ARL

A Software Tool for the Rapid Analysis of the Sintering Behavior of Particulate Bodies

by Michael C Golt, Kristopher D Behler, and Jerry C LaSalvia

NOTICES

Disclaimers

The findings in this report are not to be construed as an official Department of the Army position unless so designated by other authorized documents.

Citation of manufacturer's or trade names does not constitute an official endorsement or approval of the use thereof.

Destroy this report when it is no longer needed. Do not return it to the originator.

US Army Research Laboratory

A Software Tool for the Rapid Analysis of the Sintering Behavior of Particulate Bodies

by Michael C Golt and Jerry C LaSalvia
Weapons and Materials Research Directorate, ARL

Kristopher D Behler
SURVICE Engineering, Belcamp, MD

REPORT DOCUMENTATION PAGE

1. REPORT DATE *(DD-MM-YYYY)*	2. REPORT TYPE	3. DATES COVERED (From - To)
November 2017	Technical Report	1 June 2015–30 September 2017

4. TITLE AND SUBTITLE	5a. CONTRACT NUMBER
A Software Tool for the Rapid Analysis of the Sintering Behavior of Particulate Bodies	
	5b. GRANT NUMBER
	5c. PROGRAM ELEMENT NUMBER

6. AUTHOR(S)	5d. PROJECT NUMBER
Michael C Golt, Kristopher D Behler, and Jerry C LaSalvia	
	5e. TASK NUMBER
	5f. WORK UNIT NUMBER

7. PERFORMING ORGANIZATION NAME(S) AND ADDRESS(ES)	8. PERFORMING ORGANIZATION REPORT NUMBER
US Army Research Laboratory ATTN: RDRL-WMM-E Aberdeen Proving Ground, MD 21005	ARL-TR-8219

9. SPONSORING/MONITORING AGENCY NAME(S) AND ADDRESS(ES)	10. SPONSOR/MONITOR'S ACRONYM(S)
	11. SPONSOR/MONITOR'S REPORT NUMBER(S)

12. DISTRIBUTION/AVAILABILITY STATEMENT

Approved for public release; distribution is unlimited.

13. SUPPLEMENTARY NOTES

14. ABSTRACT

Sintering studies provide insights into how to best incorporate processing additives and optimize processing conditions to efficiently produce materials that have the desired properties and performance. The studies provide observations of the rate of densification given a thermal history, where densification is measured through dilatometry. From a series of these studies a master sintering curve (MSC) can be developed that provides the ability to predict densification of a powder and green-body process given a thermal history. The calculation of the MSC can be tedious, involving repetitive evaluations of integrals over data that need to be corrected for measurement noise and thermal expansion. As such, a software tool was developed to aid in analyzing the data acquired during the sintering studies and to readily produce MSCs. This report begins with an introduction to the software tool and its use, followed by the calculation procedures that are implemented within the tool. Last, 2 sintering studies are evaluated using the tool to validate and demonstrate the functionality.

15. SUBJECT TERMS

sintering, dilatometry, ceramic, metal, master sintering curve, alumina

16. SECURITY CLASSIFICATION OF:			17. LIMITATION OF ABSTRACT	18. NUMBER OF PAGES	19a. NAME OF RESPONSIBLE PERSON
					Michael C Golt
a. REPORT	b. ABSTRACT	c. THIS PAGE	UU	34	19b. TELEPHONE NUMBER (Include area code)
Unclassified	Unclassified	Unclassified			410-306-0946

Contents

List of Figures

iv

Acknowledgments

INTENTIONALLY LEFT BLANK.

1.   Introduction

Sintering studies are an important part of the development of novel ceramic and metallic materials. These studies provide insights into the effects of processing additives and optimize processing conditions to efficiently produce materials that are not only fully dense, but also possess microstructures that yield the desired properties and performance. The ability to predict material densification behavior for a given thermal history is an important result of sintering studies and has been made possible in part through the development of the master sintering curve (MSC) theory by Su and Johnson (1996). The MSC provides a generalized model of sintering behavior for a given powder and green-body process. It is practical for industrial use to accurately predict the densification result for a given thermal history (Pouchly and Maca 2010). Since Su and Johnson's MSC paper, further development of the MSC theory has occurred (Kiani et al. 2006; Park et al. 2006; Blaine et al. 2009) and is now routinely found in literature describing the sintering behavior of both ceramic (Ewsuk et al. 2006; Zuo et al. 2014) and metallic (Blaine et al. 2006; Park et al. 2006) powders. What makes the MSC attractive is its practicality in being able to provide quantitative predictions of the sintering process not found purely through modeling or simulation, but through experimental observations. Sintering studies provide observations of the rate of densification given a thermal history. Densification history is determined through dilatometry, often with the use of a linear variable displacement transducer (LVDT) that measures the changes in displacement of a specimen during the sintering process (Fig. 1). As the sample shrinks during densification, the displacement is observed via a change in resistance or capacitance internal to the LVDT and converted to a measure of distance, which is recorded at regular intervals on a PC. The measured displacement is a combination of linear shrinkage due to densification of the specimen and thermal expansion of the load train components. To determine the change in displacement due to the linear shrinkage of the specimen, the thermal expansion of the load train components must be subtracted from the measured displacement. The thermal expansion of the load train components is often measured separately in an experiment without the specimen but with identical thermal history.
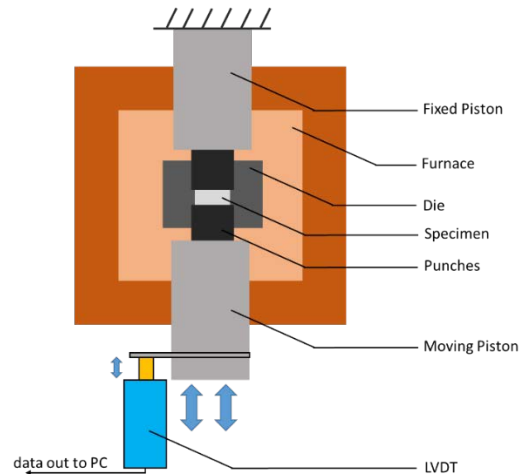
Fig. 1 **Illustration of how a dilatometer is used to measure the displacement of a specimen undergoing sintering in a hot press**

Typically a sintering study involves running a series of powder specimens, with identical green-body preparation, through different thermal histories. These thermal histories might vary in either heating rate or hold temperature. Because the specimens are prepared identically, they will have a common, apparent sintering activation energy that will repeatedly have a specific amount of densification corresponding to a specific amount of work applied. Because of differences in either heating rate or hold temperature, specimens will exhibit different densification histories, as well as densification-temperature profiles. When the densification-temperature profiles are plotted against the amount of work performed (see Section 3.5, Theta and the Master Sintering Curve), they will overlap forming the MSC. The apparent sintering activation energy is needed to calculate the work performed. Often this is unknown. The sintering study provides a means of estimating the apparent activation energy term by calculating the work performed over a range of activation energies to find the value in which the differences between all of the densification-temperature curves in the study are minimized. These calculations can be tedious, involving repetitive evaluations of integrals over data that need to be corrected for measurement noise and thermal expansion. As such, a software tool was developed to aid in analyzing sintering studies data and to readily produce the MSC. This report begins with an introduction to the software tool and its use, followed by the calculation procedures that are implemented within the tool. Last, 2 sintering studies are evaluated using the tool to validate and demonstrate the functionality.

This report provides an overview of the use of this software tool, as well as a description of the algorithms contained within the tool for calculating the densification, the apparent activation energy, and the MSC of materials sintered

with dilatometry. This report also provides a reference to the procedures and calculations used to analyze the data and serves as a guide to the proper operation of the software.

2.   Software Operational Overview and Procedures

This section introduces the software tool and its use. Figure 2 shows a screen capture of the graphical user interface. Experimental files are defined as LVDT data of processing runs containing a densifying part, whereas baseline files contain LVDT data on blank dies during a similar processing history and are used for calibration/correction of the experimental data. The users should first load experimental files by clicking the "Load Experimental Files" button, which will ask them to select the files to be imported into the program. Both single and multiple selections can be made on Excel-compatible (*.csv, *.xls, *.xlsx) files. After processing the data, the program will display the imported filenames in the experimental files list box (Fig. 2, item 1). By a similar mechanism, users can import baseline files by clicking the "Load Baseline Files" button under the baseline files list box (Fig. 2, item 2). The import process may take several minutes depending on the number of files selected, and a progress bar will be displayed during this time. After the files are loaded, single or multiple file(s) can be selected from each file name list box to display in the axes window (Fig. 2, item 3). Selecting an individual file will display the experimental conditions saved in the file in the properties list box (Fig. 2, item 4). Selecting multiple files will only display the properties for the first file selected in the multiselection. However, multiple plots of data can be displayed simultaneously in the axes window.
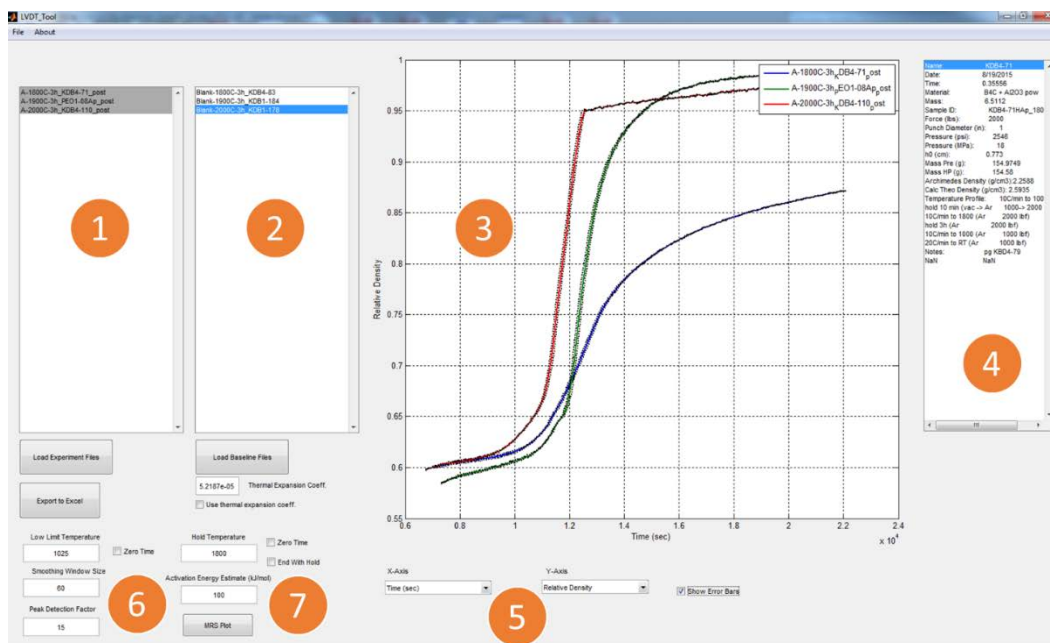
Fig. 2   Screen capture of the software tool

During the import process, the program will automatically identify all data columns included in the files (both experimental and baseline). In addition, if baseline files are loaded, the program will automatically include data columns for corrected LVDT displacement as well as a calculated relative density (ratio between actual and theoretical density). All data columns identified during the import process will be included in the x- and y-axis selection drop-down boxes (Fig. 2, item 5). Any combination of data columns can be plotted in the axes window by choosing them from these drop-down menus. Additional processing controls for the data include the ability to set the lower temperature limit of the data, the smoothing window size, and the peak detection factor (Fig. 2, item 6). These settings are described in detail in Section 3. Two checkboxes are available to zero any plot containing a time data column by either the lower limit temperature or the hold temperature. The "End With Hold" checkbox will crop the experimental data up to the end of the hold by locating the last measurement recorded at the hold temperature and returning only the data recorded before that time.

The baseline files can be used to directly remove the effects of thermal expansion as measured in a baseline run. An example of a baseline run is a blank die that includes no powder material or a die that contains fully densified material of the same composition. Alternatively, the coefficient of thermal expansion (CTE) value for the baseline run can be calculated and used to subtract the thermal expansion effects from the experimental data. If the "Use thermal expansion coeff." checkbox is checked, the CTE will be calculated from the heating side of the baseline data. If

the "Use thermal expansion coeff." box is checked and no baseline data are provided, the software attempts to determine the CTE from the cooling side (after the last measurement at the hold temperature) of the experimental data, where it is assumed that the part is fully densified and all dilatometry is due to thermal expansion of the part and die.

A file menu at the top of the program provides the ability to save and load the workspace. This feature allows the user to preserve all information on the imported files, as well as the current plot and calculation settings for future analysis.

Right-clicking on any of the plots presents an analysis menu that currently allows the user to fit a straight line to a section of the selected data, bounded by a region that the user selects via cross hairs. Future plot analysis features, such as more complicated curve fitting and modeling functions, will be added to this right-click option as they are developed. Right-clicking on any open space in the axes outside of the curves allows the user to view the plot in a new window. From here the user can modify the axes and save the figure as a picture for use in reports and presentations.

The program attempts to extract the hold temperature from the file name (see the Appendix) and will display it when the file is selected in the hold temperature text box. If the program cannot extract the temperature, or the extracted temperature is wrong, the user can change the temperature associated with the file by entering a new temperature in the text box. This temperature can be changed in the batch for both the experimental and the baseline files.

The software has the ability to attempt to determine the activation energy of a series of experiments that were recorded on the same material but at different heating rates or hold temperatures. This is accomplished by comparing the plots of the density versus $LOG_{10}(\theta)$ (see Section 3). Clicking the "MRS Plot" button (Fig. 2, item 7) will begin a search for the apparent activation energy that minimizes the mean residual squares (MRS) difference between the density/$LOG_{10}(\theta)$ curves of the selected experiments. A pop-up figure will display the progress of the search that considers 30 activation energies that are $\pm15\%$ of the estimate shown in the "Activation Energy Estimate (kJ/mol)" box. At the end of the search, the activation energy that minimizes the MRS of the density/$LOG_{10}(\theta)$ will replace the value in this box. Manually changing this value will update the calculation of the density/$LOG_{10}(\theta)$ plots.

3. Calculations

3.1 Automatic Data Cropping

The software interface was developed to provide researchers with a tool to rapidly process the data captured during the high-temperature processing of materials. During a typical thermal treatment of a material, there is a heating phase, followed by a hold phase, followed by a cooling phase. In certain experiments, there are sharp irregularities in the dilatometry data due to the application or release of a load. Data of interest are found between these discontinuities, and the software can automatically extract the data of interest for analysis. For example, at a certain relatively low temperature point in the heating phase, the pressure is increased to maximum load, leading to a discontinuity in the displacement data versus time (Fig. 3, location 1). Similarly, at the end of the hold the pressure is reduced to zero, leading to a second discontinuity (Fig. 3, location 3). The user of the software provides the lower-limit temperature, which is default to 1025 °C, at which they increase the pressure, and the software automatically identifies the high-temperature discontinuity after the hold. To find this second discontinuity, the numerical derivative of the relative displacement (*Displacement [REL]*) is calculated at all points in that data column. Thus, high-frequency changes in the displacement data will be indicated by peaks in the derivative. Then, a standard deviation of that entire derivative is found, and the first peak that exceeds that standard deviation multiplied by a factor is selected as the end point, or location 3 in Fig. 3. The user can determine the peak detection factor, which is default to 15. A low value will trigger on smaller peaks, and a higher value will tend to not trigger at all to crop the data. Data cropping is applied to both experimental and baseline data.
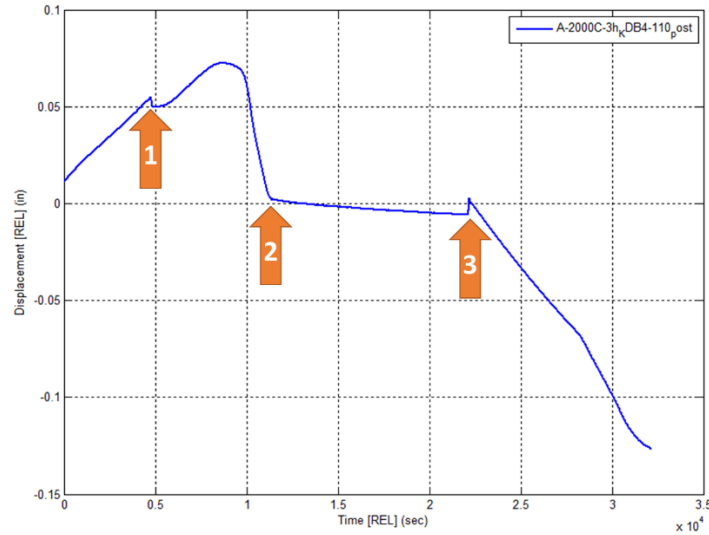
Fig. 3   Displacement data as recorded vs. time by an LVDT. Location 1 is the time where the pressure was increased—this usually coincides with a temperature. Location 2 is the time at which the hold temperature was reached. Location 3 is the time at which the hold ended and pressure was reduced.

3.2 Data Smoothing and Error Calculation

The displacement data measured by the LVDT can be noisy. A smoothing function is automatically applied to data columns relating to the displacement measurement. The algorithm used to smooth the data is based upon a moving average with a window size that is user adjustable. A similar moving standard deviation calculation is used to help determine a confidence interval for the smoothed data, as well as subsequent transforms and calculations based upon the smoothed data. The default for the window size is 60 data points. A setting of 1 will result in the original signal without any smoothing. The automatic data cropping is performed on the smoothed displacement signal, thus changing the window size may also change the peak detection. This smoothing step and error calculation are performed on both experimental and baseline files.

3.3 Displacement Correction

Baseline LVDT data collected on a blank die that underwent the same thermal history as the experimental LVDT data can be used to calibrate the experimental displacement signal by removing artifacts such as thermal expansion of the die and the measurement system. If baseline data are loaded into the program, it is automatically linked to the proper experimental files by the common hold temperature. There are 2 ways in which the baseline displacement data can be used to correct the experimental displacement. The first is to use the baseline

displacement versus temperature data to calculate the combined CTE of the die and the measurement system. The displacement due to thermal expansion at each recorded temperature is subtracted from the experimental displacement curve to obtain a corrected displacement. The CTE correction will occur if the "Use thermal expansion coeff." is checked. This method does not require the baseline run to have the same ramp rate, hold time, or sampling rate; however, a baseline file is linked to the experimental file through a common hold temperature. The second method is to use the baseline displacement data to perform a direct subtraction from the experimental displacement data at each recorded time step. This assumes that baseline data was performed with identical ramp rates and measurement sampling rates, which is essential for proper calibration. The low-limit temperature value is used to sync the beginning of the experimental and baseline data streams. A calibrated experimental data stream is then found by subtracting the baseline displacement data from the experimental displacement data ($d_{corrected} = d_{experimental} - d_{baseline}$). This calculation is performed on the individually cropped and smoothed experimental and baseline relative displacement data stream (*Displacement [REL]*). If no corresponding baseline file is provided or available, the software will attempt to use the CTE calculated from the cooldown phase of the experimental data. Since there is uncertainty in the data introduced by smoothing the curves via a moving average filter, the total standard deviation due to smoothing for the corrected displacement calculation is found as the sum of each curve's moving standard deviation ($\sigma_{total} = \sigma_{experimental} + \sigma_{baseline}$). There is a checkbox below the axes window that toggles the display of the data uncertainty. When checked, the plot will overlay the 95% confidence bounds, which are calculated as $2\sigma_{total}$. If the CTE value is used, the experimental standard deviation ($\sigma_{experimental}$) is the total standard deviation (σ_{total}). An example of the input and output displacement curves, along with the 95% confidence bounds, is shown in Fig. 4.
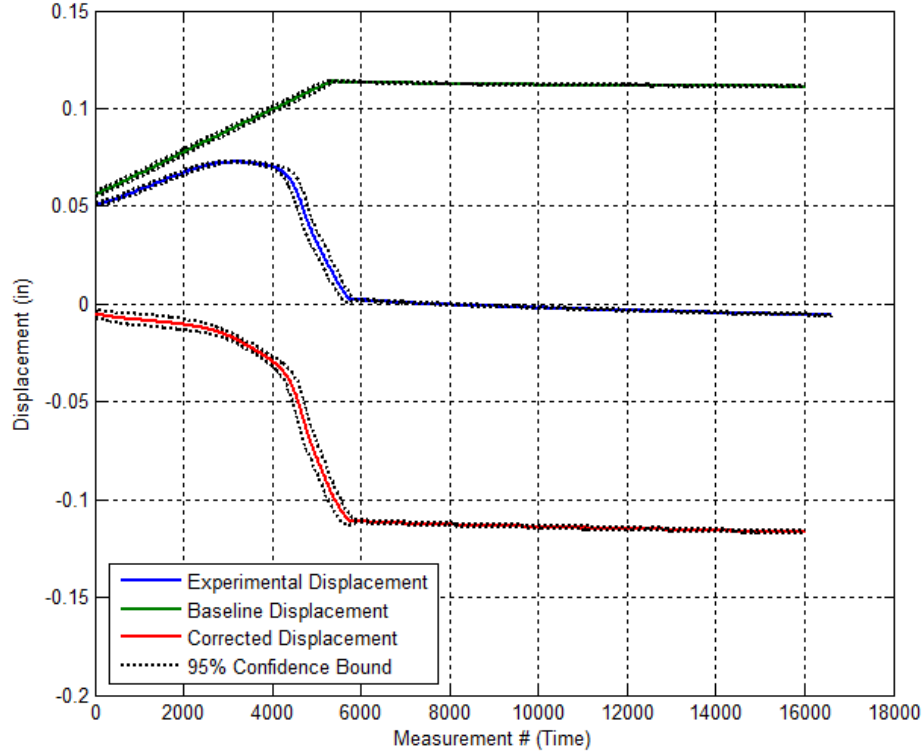
Fig. 4 **Illustration of a baseline LVDT displacement curve used to correct an experimental LVDT displacement curve. The 95% confidence bounds due to uncertainty arising from data smoothing are calculated and displayed.**

3.4 Percent Theoretical Density

One objective of recording LVDT data during the processing of a material is to calculate the density of the specimen at any instant during the thermal profile. A ratio between the density of the part and the theoretical density throughout the processing run can be calculated by using the baseline-corrected displacement data ($d_{corrected}$), the initial height of the powdered sample (h_0), the initial mass of the sample (m), the area of the die (A_0), the initial density (ρ_0), the calculated theoretical density (ρ_c), the measured final density of the sample (ρ_m), the final thickness of the sintered part (h_f), and the final area of the sintered part (A_f). The initial density ρ_o and density ρ at any instant of time are related by the following relationship:

$$\rho = \frac{\rho_o}{V/V_o},$$ (1)

where V_o is the initial sample volume and V is the sample volume at any instant of time. For cylindrically shaped samples that remain cylindrical during densification, V_o/V is given by

$$\frac{V}{V_o} = \left(\frac{h}{h_o}\right)\left(\frac{A}{A_o}\right) = \left(\frac{h}{h_o}\right)\left(\frac{R}{R_o}\right)^2 = \left(\frac{h_o - \Delta h}{h_o}\right)\left(\frac{R_o - \Delta R}{R_o}\right)^2 = \left(1 - \frac{\Delta h}{h_o}\right)\left(1 - \frac{\Delta R}{R_o}\right)^2, \qquad (2)$$

where h and R are the instantaneous height and radius of the sample, respectively. These are related to the initial height and radius of the sample by $h = h_o - \Delta h$ and $R = R_o - \Delta R$, where Δh and ΔR are the change in sample height and radius.

For isotropic or uniform shrinkage (i.e., $\Delta R/R_o = \Delta h/h_o$), which is characteristic of pressureless sintering of homogeneous green bodies, Eq. 2 simplifies to

$$\frac{V}{V_o} = \left(1 - \frac{\Delta h}{h_o}\right)^3. \qquad (2a)$$

Substituting Eq. 2a into Eq. 1 yields the following relationship for instantaneous density ρ assuming uniform shrinkage:

$$\rho = \frac{\rho_o}{\left(1 - \dfrac{\Delta h}{h_o}\right)^3}. \qquad (1a)$$

For the case of uniaxial hot-pressing where the volume change is dominated by the change in sample thickness h (i.e., $\Delta R = 0$ in Eq. 2), Eq. 1 becomes

$$\rho = \frac{\rho_o}{\left(1 - \dfrac{\Delta h}{h_o}\right)}. \qquad (1b)$$

For the more general case where the change in sample thickness and radius varies in such a way not easily related, such as in constrained sintering and sinter forging (i.e., where sintering is constrained in one or more directions or pressure is applied in only one direction), Eq. 2 must be used with Eq. 1 to determine the instantaneous density ρ. However, under the assumption of uniform densification in time, a simple expression can be derived for this more general case. Under this assumption, the change in volume can be expressed as

$$\frac{V}{V_o} = \left(\frac{h}{h_o}\right)\left(\frac{A}{A_o}\right) = \left(1 - \frac{\Delta h}{h_o}\right)\left(1 - \frac{\Delta A}{A_o}\right) \cong \left(1 - \frac{\Delta h}{h_o}\right)\left(1 - \alpha\frac{\Delta h}{h_o}\right), \qquad (2b)$$

where it is assumed that $\Delta A/A_o$ is proportional to $\Delta h/h_o$ with α being the proportionality constant given by

$$\frac{\Delta A}{A_o} = \alpha\frac{\Delta h}{h_o} \rightarrow \alpha = \frac{\Delta A/A_o}{\Delta h/h_o} = \frac{(A_f - A_o)/A_o}{(h_f - h_o)/h_o} = \frac{(A_f/A_o - 1)}{(h_f/h_o - 1)}, \qquad (3)$$

where A_f and h_f are the final area and height of the sample. The expression for the instantaneous density ρ becomes for this condition:

$$\rho = \frac{\rho_o}{\left(1-\dfrac{\Delta h}{h_o}\right)\left[1-\dfrac{\left(A_f/A_o-1\right)}{\left(h_f/h_o-1\right)}\dfrac{\Delta h}{h_o}\right]} \cdot \qquad (1c)$$

For unconstrained pressureless sintering and uniaxial hot-pressing, Eq. 1c simplifies to Eqs. 1a and 1b, respectively. Here, the change in density is related to a change in the volume. The height change in the denominator is cubed since in isotropic shrinkage a linear change in one dimension should be the same in the other dimensions of the cubic measure of volume. For instances where isotropic shrinkage is assumed, a real-time and online calculation of the density can be calculated from the dilatometer reading during processing. In cases where pressure is applied or the shrinkage is not isotropic, an area cannot be assumed from a measure of the shrinkage in the height unless the ratio of the change in area given a change in height is known. The initial and final sample dimensions are used to obtain a shrinkage, an area to thickness ratio (r), for the instances that the volume shrinkage is not isotropic. Here, r is calculated as

$$r = \frac{A_o - A_{end}}{h_0 - h_{end}} \cdot \qquad (4)$$

When pressure is applied during densification, the area will remain the same from beginning to end and $r = 0$. If no end dimension data are provided, the software will assume that the densification was pressure-assisted and set $r = 0$. The density at each recorded time step, $\rho(t)_{LVDT}$, is then calculated from the corrected displacement and compared to the theoretical density as a ratio via the following:

$$\rho(t)_{LVDT} = \frac{\rho_0}{\left(1-\frac{\Delta A}{A_0}\right)\left(1-\frac{\Delta h}{h_0}\right)} = \frac{\frac{m}{A_0 h_0}}{\left(1-\frac{r(h_0-h_t)}{A_0}\right)\left(1-\frac{(h_0-h_t)}{h_0}\right)}$$

$$where\ h_t = h_0 + d(t)_{corrected} \qquad (5)$$

$$\frac{\rho(t)_{LVDT}}{\rho_c} = \frac{\rho(t)_{LVDT}}{\rho_c} \cdot \frac{\rho_m}{\rho(t=end)_{LVDT}}$$

The part density ($\rho(t)_{LVDT}$) is found at all times (t) of the processing run, and the ratio between the part density and the theoretical density is normalized by the ratio between the Archimedes' density and the part density at the end of the hold. This normalization is performed, in part, to correct for mass loss from volatilization. The constants needed to perform the density calculations are supplied in the experimental file and are automatically extracted by the program. The uncertainty

in the corrected displacement data is propagated through the density calculation as a function of processing time by adding the displacement total standard deviation (σ_{total}) to the corrected displacement ($d(t)_{corrected}$) in Eq. 5. An upper bound to the density is found when a positive signed σ_{total} is used, and a lower bound is found when a negative signed σ_{total} is used. These bounds can be overlaid on the theoretical density ratio by clicking the "show error bars" box under the axes window. An example of the density ratio and the confidence bounds is shown in the axes window of Fig. 2, item 3.

3.5 Theta and the Master Sintering Curve

Su and Johnson (1996) developed the concept of an MSC that characterizes the sintering behavior of a given powder prepared by a given green processing, regardless of the heating profile. They formalize the MSC of a powder from the combined stage sintering model where the densification rate, which is proportional to the linear shrinkage rate, is related to the dominant atomic diffusion process and the microstructural and material properties; Eq. 6 shows this relation. On the left-hand side of this relation are terms associated with the microstructural evolution, where G is the mean grain diameter, and Γ is used to relate the instantaneous linear shrinkage rate to the diffusion coefficient and other material and geometric properties. The right-hand side are the terms related to the atomic diffusion process, where ρ is the density, γ is the surface energy, Ω is the atomic volume, D_0 is a coefficient related to either the volume (where $n = 3$) or grain boundary diffusion (where $n = 4$), Q is the apparent activation energy, and T is the absolute temperature.

$$\int_{\rho_0}^{\rho} \frac{(G(\rho))^n}{3\rho\Gamma(\rho)} d\rho = \int_0^t \frac{\gamma\Omega D_0}{kT} \exp\left(-\frac{Q}{RT}\right) dt \ . \tag{6}$$

Su and Johnson then define theta, θ, as the right-hand side, which is dependent only on Q and the time-temperature profile and is therefore related to the amount of sintering work applied:

$$\theta(t, T(t)) = \int_0^t \frac{1}{T} \exp\left(-\frac{Q}{RT}\right) dt \ . \tag{7}$$

An MSC is then obtained empirically by plotting the density, as obtained from the dilatometry data, versus the integration of Eq. 7 with a known or approximated Q. Because θ is dependent upon the work done on the powder, and independent of the microstructure and properties, it can be used to predict the sintering results (density) given any time-temperature history through the MSC.

3.6 Finding the Apparent Sintering Activation Energy

A given powder and green-body process will have a consistent apparent sintering activation energy, Q, that will result in a consistent MSC (density versus θ) regardless of the time-temperature profile used to densify. When the activation energy used in the calculation of θ is correct, data from samples undergoing different sintering paths will converge onto a single curve in the density versus θ plot, the MSC. This aspect of the MSC can be used to find the apparent activation energy when it is not known a priori. To do this, a series of usually 3 to 5 heating histories with different time-temperature relationships are run on a given powder and green-body process. The MSCs for each heating history are calculated using an estimate of Q. Since the correct value of Q will result in the convergence of all data points onto a single curve, the mean of the residual squared difference (Eq. 8) between the MSCs can be calculated to determine which value of Q results in the least difference between the curves. The apparent activation energy can be estimated from locating the minima in a plot of the MRS over a range of estimated activation energies. The MRS for this is calculated over the relative densities between 0.65 and 0.9. This range is chosen as it is the most linear portion of the curves, where small changes in θ result in large changes in density.

$$MRS = \sqrt{\frac{1}{\rho_f - \rho_0} \int_{\rho_0}^{\rho_f} \frac{\sum_{i=1}^{N}\left(\frac{\theta_i}{\theta_{avg}} - 1\right)^2}{N} d\rho} \, , \qquad (8)$$

where N is the number of curves, θ_{avg} is the average MSC, and ρ_0 and ρ_f are the low and high limits of the density range over which the MRS is calculated.

4.   Experimental Results

4.1 Model Data to Validate Calculations

To validate the operation and calculations of the software, a model sintering dataset on alumina was obtained from Su and Johnson's (1996) seminal paper on the derivation of the MSC. To develop this model dataset, specimens were rapidly heated at 1 °C/s to 750 °C and then to 1500 °C at constant heating rates of 8 °C, 15 °C, 30 °C, and 45 °C/min in an oxygen atmosphere. Since the software imports data files containing the LVDT displacement over time and temperature, the density versus temperature curves reported by Su and Johnson were used to construct artificial dilatometer displacement data assuming isotropic shrinkage (Eq. 1a). Furthermore, a simulated thermal expansion of a die and measurement system was added to the displacement data with a CTE of 2.3622E-6, and a corresponding

simulated baseline data file was generated. The software imported the simulated experimental and baseline data files, and the calculated relative density versus temperature curves (Fig. 5) are in accordance with the model dataset of Su and Johnson. Next, the calculation of the MSCs for the thermal histories was performed, and the apparent sintering activation energy was found as the minimum in the MRS plot (Fig. 6). A value of 455 kJ/mol was obtained using this method, which is in agreement with the value of ~440 kJ/mol obtained by Su and Johnson, where they expected to obtain a value of 488 kJ/mol. When the value of 455 kJ/mol is used, the MSCs for all 4 heating histories converge, and the values of θ are in agreement with Su and Johnson.
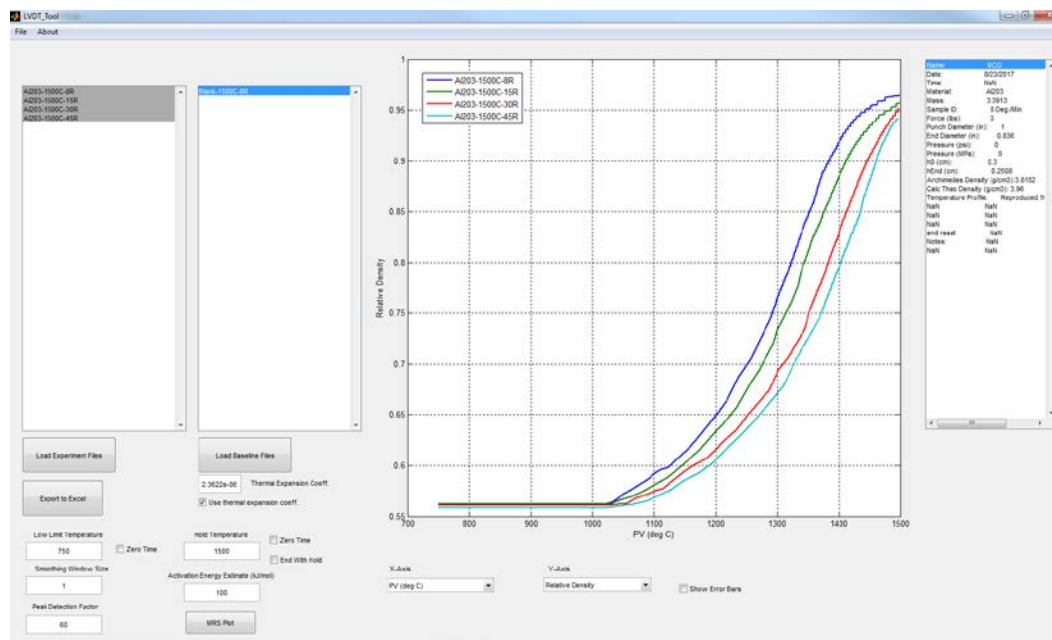

Fig. 5   Calculated relative densities from simulated dilatometry data files generated from the model study on alumina by Su and Johnson (1996)
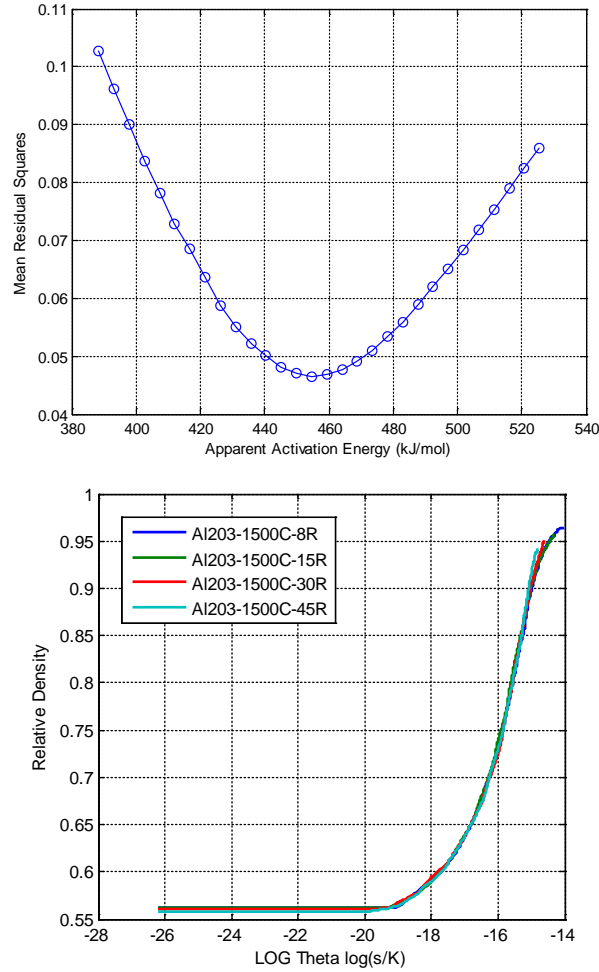
Fig. 6   (Top) MRS calculation to find an apparent activation energy of 455 kJ/mol for the model study on alumina by Su and Johnson (1996). (Bottom) MSC curves are in agreement when calculated with the activation energy of 455 kJ/mol.

4.2 US Army Research Laboratory (ARL) Sintering Experimentation

Specimens of Baikalox SM-8 (Baikowski, Charlotte, NC) alumina powder were prepared within a 1-inch-diameter graphite die, with a boron nitride coating on the punches and dies. Then 3.3 g of powder were added to the die in an attempt to achieve a green thickness of 3.3 mm when the die was uniaxially pressed at 82.7 MPa before sintering. The green density was calculated from the powder mass and the geometry of the powder in the die. The die was then transported to a vacuum furnace with uniaxial pistons that were held in contact to the die using the vacuum. A dilatometer was used to record the shrinkage of the part during 3 heating profiles of 5 °C, 10 °C, and 15 °C/min to a hold temperature of 1450 °C. The specimens were maintained in the hold until the dilatometer registered no further displacement, indicating a densified microstructure. The specimens were cooled to room temperature at the

same rate in which they were heated. A helium pycnometer was used to measure the final density. A baseline experiment was performed using a blank die following the same heating profile as the 10 °C/min specimen. From this baseline, a CTE of 6E-6 was calculated from the baseline data and used to correct the displacement data from the specimen experiments. The specimens did not show isotropic shrinkage, and as such, the final area and thickness were used to calculate the area-to-thickness ratio that was used to correct the area change given a measured thickness change. Nonisotropic shrinkage was likely caused by nonideal sintering pressure delivered to the thickness of the part through the vacuum pull-in of the uniaxial pistons in the furnace. The calculated densities relative to a theoretical density of 3.986 g/cc for the 3 heating profiles are shown in Fig. 7. The initial relative densities as calculated via Eq. 5 are overestimated by 10% for the 10 °C/min profile, and 4% for the 5 °C/min profile. This is likely due to normalizing the relative density calculation by the measured final density. For these histories, the specimen may have continued to densify after the hold during the cooldown. Therefore, if the data up to the end of the hold is scaled according to the assumption that it ended with the density as measured after the specimen was removed from the die, it will have the effect of shifting the relative density higher at all points. Extreme hold times to ensure complete densification or rapid cooling to avoid further densification post-hold may help to eliminate this problem. The apparent sintering activation energy was found to be 343 kJ/mol by finding the minimum in the MRS plot over a range of frequencies (Fig. 8). This value for the activation energy is lower than the reported values for the alumina powder and method used by Su and Johnson. The lower activation energy for the Baikowski powder used for this study is expected, as it is marketed as having a high sinterability and has a smaller initial grain size than the powder used by Su and Johnson.
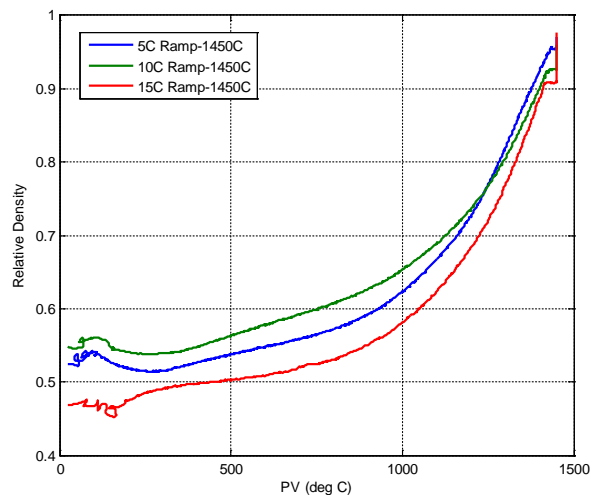

Fig. 7   **The calculated relative densities vs. temperature of the SM-8 alumina specimens**
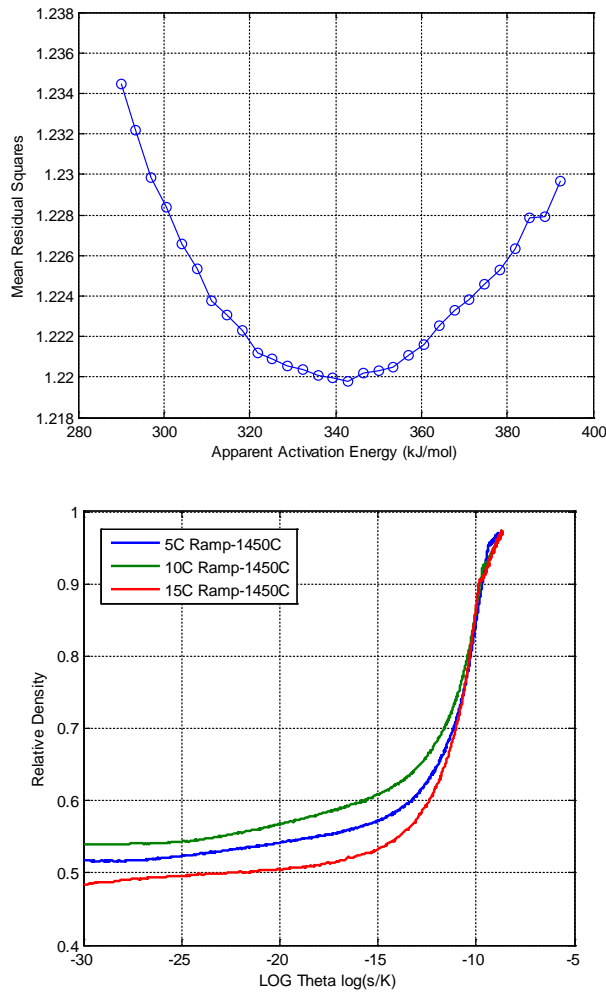
Fig. 8   (Top) MRS calculation to find an apparent activation energy of 343 kJ/mol for the thermal histories on SM-8 alumina. (Bottom) MSC curves are in agreement for the range of relative densities between 0.65 and 0.9 when calculated with the activation energy of 343 kJ/mol.

5.   Conclusions

A procedure for analyzing dilatometry data obtained during the sintering of materials has been developed and implemented through a new software tool. This tool allows for the rapid processing, visualization, and analysis of a series of thermal history data. The major utility of this analysis is the ability to determine the instantaneous density of specimens undergoing sintering, as well as the ability to determine the apparent sintering activation energy of a series of thermal histories, resulting in an MSC for a given powder and green-body process. This procedure, which includes importing data, automatic data cropping, correction and smoothing calculations, and MSC development, has been validated through its agreement with results found in literature. Once an MSC is obtained, it can be used to predict the

sintering behavior of a given material and green-body process to efficiently obtain desired microstructures. The sintering activation energies of materials are an important material property; they are critical for understanding material processing behavior and are therefore also useful to the public discourse. These procedures are currently implemented in several ARL mission programs focused on the development of novel ceramic materials and novel processing methods.

6. References

Blaine DC, Gurosik JD, Park SJ, German RM, Heaney DF. Master sintering curve concepts as applied to the sintering of molybdenum. Metallurgical and Materials Transactions A. 2006;37(3):715–720.

Blaine DC, Park SJ, German RM. Linearization of master sintering curve. Journal of the American Ceramic Society. 2009;92(7):1403–1409.

Ewsuk KG, Ellerby DT, DiAntonio CB. Analysis of nanocrystalline and microcrystalline ZnO sintering using master sintering curves. Journal of the American Ceramic Society. 2006;89(6):2003–2009.

Kiani S, Pan J, Yeomans JA. A new scheme of finding the master sintering curve. Journal of the American Ceramic Society. 2006;89(11):3393–3396.

Park SJ, Martin JM, Guo JF, Johnson JL, German RM. Grain growth behavior of tungsten heavy alloys based on the master sintering curve concept. Metallurgical and Materials Transactions A. 2006;37(11):3337.

Pouchly V, Maca K. Master sintering curve: a practical approach to its construction. Science of Sintering. 2010;42(1):25–32.

Su H, Johnson DL. Master sintering curve: a practical approach to sintering. Journal of the American Ceramic Society. 1996;79(12):3211–3217.

Zuo F, Badev A, Saunier S, Goeuriot D, Heuguet R, Marinel S. Microwave versus conventional sintering: estimate of the apparent activation energy for densification of α-alumina and zinc oxide. Journal of the European Ceramic Society. 2014;34(12):3103–3110.

INTENTIONALLY LEFT BLANK.

Appendix. Appropriate Input File and Naming Format

Adhering to a specific file format is critical for this program to work. An example of the proper data-file format is shown in Fig. A-1, where all highlighted labels and columns must be included and have the same syntax (spelling and punctuation). As shown in this example, other data columns can be included and will be recognized by the program for display as well as other experimental notes in the header section. A 2-column header must be included prior to the data listing and must contain the required labels in the first column of the spreadsheet, with the related data in the second column. Following the header section is a row containing data column titles, which must include the highlighted columns. This header row must begin in column 1 of the spreadsheet. All data then follow in the subsequent rows. A "NaN" should be used where data are not available and will be ignored by the program.

The filenames for both the experimental and baseline files should follow a convention where "-2000C-" is included to indicate the hold temperature. The dashes (-) used in the convention need to be the first and second dashes used in the filename to be autorecognized by the software. A "C" or "F" must also be included following the hold temperature. For example, the file name "A-2000C-3h_KDB4-110_post" is appropriate, and the hold temperature of 2000 °C will automatically be extracted from the filename. If the software fails to properly recognize the hold temperature, a value of 0 °C will be used and can later be modified in the program to the appropriate temperature (see Section 2, Software Operational Overview and Procedures, in the main body of this report).

Name:	KDB					
Date:	6/8/2017					
Time:	10:28 AM					
Material:	Al2O3					
Mass:	3.3218					
Sample ID:	Al2O3 5°C/min					
Force (lbs):	0					
Punch Diameter (in):	1					
End Diameter (in):	0.85669					
Pressure (psi):	0					
Pressure (MPa):	0					
h0 (cm):	0.328					
hEnd (cm):	0.233					
Archimedes Density (g/cm3):	3.8649					
Calc Theo Density (g/cm3):	3.986					
Temperature Profile:	RT->1450°C @ 5°C/min					
hold until dense						
1450°C-> RT @ 5°C/min						
Notes:						
Time (sec)	Time [REL] (sec)	Displacement [ABS] (in)	Displacement [REL] (in)	Vacuum (Torr)	PV (deg C)	WSP (deg C)
0	NaN	0.50169178	0.50169178	NaN	21	1
1	NaN	0.5008606	0.5008606	NaN	21	1
2	NaN	0.50083684	0.50083684	NaN	21	1
3	NaN	0.50081587	0.50081587	NaN	21	1
4	NaN	0.50084351	0.50084351	NaN	21	1
5	NaN	0.50082857	0.50082857	NaN	21	1

Fig. A-1 Example of the proper data-file format. Highlighted labels and columns must be included and of the same syntax.

Exporting Data

The raw and calculated data for the experimental files can be exported from the program by clicking the export button beneath the experimental files list box. The user is prompted for a save folder location, and all files currently selected will be exported to an Excel file (.xlsx) with "-Processed" added to the end of the filename as displayed in the list box. The program will attempt to export a data column for each option listed in the x- and y-axis drop-down menus, as these contain all the possible raw and calculated data fields. In addition, the program will export the experiment properties shown in the properties window along with the cropping and smoothing conditions as header information in the Excel sheet. The export will include all standard deviation calculations as well as the 2 zeroed time possibilities. The export process can take several minutes depending upon how many files are to be exported; a progress bar will be shown during the process.

List of Symbols, Abbreviations, and Acronyms

ARL   US Army Research Laboratory

CTE   coefficient of thermal expansion

LVDT   linear variable displacement transducer

MRS   mean residual squares

MSC   master sintering curve

PC   personal computer

1 (PDF)	DEFENSE TECHNICAL INFORMATION CTR DTIC OCA

2
(PDF)
	DIR ARL
	IMAL HRA
	  RECORDS MGMT
	RDRL DCL
	  TECH LIB

1 (PDF)	GOVT PRINTG OFC A MALHOTRA

3
(PDF)
	ARL
	RDRL WMM E
	  M GOLT
	  K BEHLER
	  J LASALVIA

INTENTIONALLY LEFT BLANK.